Energy-Efficient Motion Planning for Mobile Robots

Yongguo Mei, Yung-Hsiang Lu, Y. Charlie Hu, and C.S. George Lee
School of Electrical and Computer Engineering, Purdue University
{ymei, yunglu, ychu, csglee}@purdue.edu

Abstract— This paper presents a new approach to find energy-efficient motion plans for mobile robots. Motion planning has two goals: finding the routes and determining the velocities. We model the relationship of motors' speed and their power consumption with polynomials. The velocity of the robot is related to its wheels' velocities by performing a linear transformation. We compare the energy consumption of different routes at different velocities and consider the energy consumed for acceleration and turns. We use experiment-validated simulation to demonstrate up to 51% energy savings for searching an open area.

I. INTRODUCTION

Mobile robots usually carry their energy sources, such as batteries, so conserving energy is important. A robot's energy consumption can be divided into two major parts: electrical and mechanical. The former is the energy consumed by the on-board computer. The latter considers the energy consumed by the robots' motors and actuators. This paper focuses on minimizing the mechanical energy. Energy conservation can be achieved in several ways, for example, using energy-efficient motors, finding better routes, or avoiding frequent accelerations and turns. A motion plan includes a path plan and a velocity schedule. The path plan specifies the route from a source to one or more destinations. The velocity schedule decides the accelerations, velocities, and decelerations along the route. One example of velocity scheduling is using cruise control on a highway: by avoiding sudden accelerations, the vehicle's fuel efficiency can be improved.

In this paper, our goal is determining which motion plans are more energy-efficient. We compared the energy consumption of different paths at different velocities. We present a sixth-degree polynomial to model a DC motor based on our experimental data. We use linear transformations to describe the relationship between a robot's velocity and its motors' velocities. We calculate the energy consumption of different paths by considering turns, accelerations, and peak velocities. Our study is

both theoretical and practical. Our approach is different from existing studies because: (i) Our experimental data indicate that electromagnetic theory is insufficient in modeling motors' power. (ii) We distinguish a robot's velocity and its motors' velocities because they may be different; hence, our approach is more general than existing methods. (iii) We include the energy for turns and accelerations. We formulate a general problem in motion planning and use a commercial robot to experimentally validate our approach. We use an experiment-validated simulator and show up to 51% energy savings.

II. PREVIOUS WORK

Energy conservation can be achieved in several ways, for example, using energy-efficient motors [1] [4]. After the motors are chosen, energy can be saved by choosing routes and setting the velocities. For example, if a robot has to visit several places, the route can be arranged to reduce the total traveled distance (similar to traveling salesperson problem, TSP) and to avoid sharp turns that requires decelerations and accelerations. Barili et al. [3] described the concept of controlling the velocities to save energy for a mobile robot. Their work did not discuss the relationship between path planning and velocity control. Hwang et al. [9] surveyed the methods for motion planning but did not discuss energy conservation. Katoh et al. [10] presented an approach for energy conservation by creating elliptic paths but they focused on space manipulators for flying robots. Some energy-conserving techniques were designed for specific robots. For example, Silva et al. [15] analyzed the energy consumption of walking robots by controlling the locomotion variables. Yamasaki et al. [18] developed control algorithms to reduce the energy consumption of humanoid robots. Both work focused on energy consumption of walking robots. Redi et al. [13] reduced the communication energy among a group of robots; the study did not consider the energy consumed by motors. Kim et al. [11] presented a control method for industrial manipulators to minimize a weighted time-

fuel cost function. They assumed that motors' power was proportional to the drive torque and did not consider the loss due to armature resistance or mechanical friction. Li et al. [12] showed that parallel manipulators were more energy-efficient than serial manipulators in similar configurations. They considered the armature resistance loss and friction loss when they computed the energy consumption. Their calculation did not include the energy consumed by the control circuits. Duleba et al. [6] discussed nonholonomic energy-efficient motion planning based on the Newton algorithm. They took the square of control signal as the objective function; their work was theoretical without experimental validation. Our method differs from previous work because we consider the power consumed by motors' control circuits. We distinguish a robot's motion from it motors' velocities by using a linear transformation to describe their relationship. Finally, our approach is analytical and experimental.

III. ENERGY-EFFICIENT MOTION PLANNING

A. Problem Description

Consider a mobile robot that has to visit several places. These places can form a graph: each vertex is a place to visit and the edges represent the energy consumption between vertices. Path planning determines the order to visit these vertices (i.e. route). Velocity scheduling specifies the velocities and accelerations between the vertices. Path planning is more difficult than TSP. In TSP, the cost between two vertices is fixed. In contrast, the energy consumption along an edge depends on the robot's velocities. Moreover, the velocities also depend on the route. For example, if a shorter route contains several sharp turns, the robot may consume more energy due to frequent decelerations, changes of directions, and accelerations. A longer route may require less energy if the robot does not have to accelerate often. Many studies have been devoted to finding paths for mobile robots. Thus, we assume that a path planning algorithm can find several candidate paths. This paper focuses on comparing the energy of these paths.

B. DC Motors' Power Models

DC motors are frequently adopted in robots so we focus on DC motors in this paper. Let $P_m(\omega, \alpha)$ be the power consumption of a motor when it revolves at angular velocity ω with angular acceleration α ($\alpha = \frac{d\omega}{dt}$). The value of P_m depends on many factors, including the back electric and magnetic fields (EMF), armature inductance, and armature resistance. From the theory of electromagnetics, $P_m(\omega, \alpha)$ of a basic DC motor can be modeled as a second-degree polynomial of ω and

α. For many DC motors, the effect of accelerations is negligible [7] [10]. Our experimental data show that a second-degree polynomial is insufficient to closely model a DC motor's power. This is because a typical DC motor also contains an internal control circuit. Figure 1 is an example of a DC motor (MS492MH by Mr Robot Inc.). From this figure, we can see that a sixth-degree polynomial is a better model than a second-degree polynomial. The average relative error is decreased from 3.63% to 1.59%. We chose a six-degree model because it can closely approximate the experimental data without significantly more computation. Figure 1 shows the energy cosmuption per radian of the motor. From this figure, we can see that a higher angular velocity is more energy-efficient.
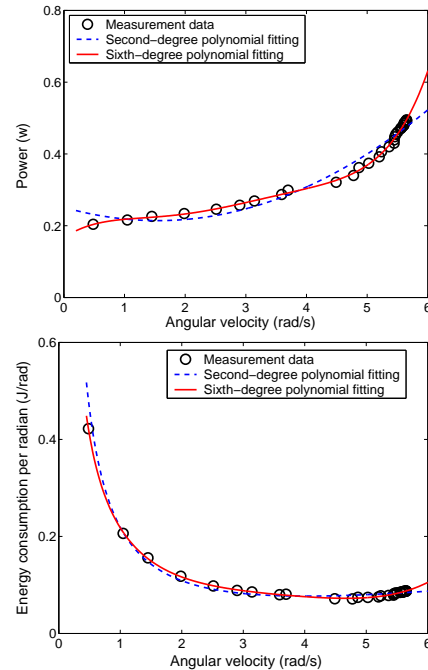

Fig. 1.   Power and energy efficiency at different angular velocities.

C. Robot's Velocity and Power Consumption

A robot usually has multiple motors and each motor drives a wheel. A wheel's velocity is the product of the wheel's radius r and the controlling motor's angular velocity ω. The velocities of a robot's wheels are not equivalent to the velocity of the robot itself. Consider a robot on a two-dimensional surface. We can represent its velocity by three variables: V_x, V_y, and Ω, as illustrated in Figure 2. In this figure, the robot is represented by a triangle. The three-element vector $< V_x, V_y, \Omega >$ represents the robot's linear and angular velocities (when
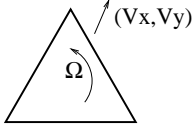
2

Fig. 2. A robot's velocity can be represented by (V_x, V_y, Ω). The value of Ω is the angular velocity when the robot is turning.
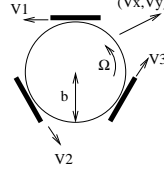

Fig. 3. The robot's velocity (V_x, V_y) is controlled by the three wheels' velocities.

the robot is turning). We use upper-case letters (V_x, V_y, and Ω) to represent the velocity of the robot and lower-case letters for the motors. If the robot is in three-dimensional space, we need to add V_z and two more angular velocities.

Omnidirectional robots are one particular type or robots that can change directions at their current locations [5] [16]. Figure 3 is an example of a three-wheel omnidirectional robot [14]. The three wheels are mounted at distance b. By adjusting the wheels' velocities, the robot can move in any direction. If a robot is omnidirectional, it can turn ($\Omega \neq 0$) without moving ($V_x = V_y = 0$). Let v_1, v_2, and v_3 be the velocities of the three wheels. The relationship between the robot's velocity and the wheels' velocities can be expressed by [14]

$$\begin{pmatrix} v_1 \\ v_2 \\ v_3 \end{pmatrix} = \begin{pmatrix} -1 & 0 & b \\ \frac{1}{2} & -\frac{\sqrt{3}}{2} & b \\ \frac{1}{2} & \frac{\sqrt{3}}{2} & b \end{pmatrix} \begin{pmatrix} V_x \\ V_y \\ \Omega \end{pmatrix} \quad (1)$$

This type of relationship is not restricted to the robot shown in Figure 3. Linear transformations are also used in other types of robots, such as a differential robot [2] or a four-wheel omnidirectional robot [5]. Suppose a robot has k motors and the velocity of the ith wheel is v_i. We can find a transformation to describe the relationship between v_i and $< V_x, V_y, \Omega >$. This relationship is called the robot's manipulator Jacobian [8]. We control the robot's velocity $< V_x \ V_y \ \Omega >$ by adjusting the motors' velocity $< v_1 \ v_2 \ ... \ v_k >$.

$$\begin{pmatrix} v_1 \\ v_2 \\ v_3 \\ ... \\ v_k \end{pmatrix} = J \begin{pmatrix} V_x \\ V_y \\ \Omega \end{pmatrix} \quad (2)$$

Let $V(t) = < V_x(t), V_y(t), \Omega(t) >$ be the robot's velocity at time t. The ith wheel's velocity is $v_i(t) = J_{i,1}V_x(t) + J_{i,2}V_y(t) + J_{i,3}\Omega(t)$. Suppose all wheels have the same radius. The motors' angular velocities is

the wheels' velocities divided by the radius, r, of the wheels. The robot's power consumption is the sum of all k motors' power:

$$\sum_{i=1}^{k} P_m\left(\frac{v_i(t)}{r}, \frac{1}{r}\frac{dv_i(t)}{dt}\right) \quad (3)$$

D. Search Problem in An Open Area
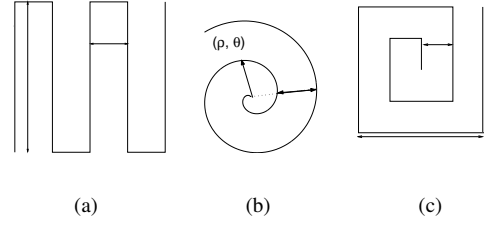

(a)   (b)   (c)

Fig. 4. (a) scan lines (b) spiral, and (c) square spiral.

We consider a search task to covers an open area, such as a robot for automatic floor cleaning. Suppose a robot that can clean a square tile of area $(2l)^2$ (l from the robot's center to each side). The robot can clean the area in different ways. In this paper, we compare three cleaning strategies: scan lines, spirals, and square spirals. Figure 4 shows these strategies. Using the scan-line strategy, the robot starts from one corner and moves at a constant velocity until it reaches the boundary. Then, the robot turns $90°$, moves $2l$, turns $90°$, and moves at a constant velocity again. The distance between two scan lines is $2l$ so that the robot can cover the whole area. With the spiral strategy, the robot follows a curve whose radius continuously increases. Using the polar coordinate, the radius linearly increases as the angle increases. When the robot moves around an angle of 2π, the radius increases by $2l$. Therefore, the radius ρ can be expressed as $\rho = \frac{2l}{2\pi}\theta = \frac{l}{\pi}\theta$. Square spirals are similar to spirals: the robot moves around the center and the traveled distance increases after the robot moves 2π around the center. The difference is that the robot moves along straight lines, not curves, for square spirals and have $90°$ turns. Notice that the robot starts from the center for the spirals and the square spirals. In contrast, in the scan lines the robot starts from one corner. Also, the covered shapes are different. Since our focus is calculating the energy per unit area, we do not consider these difference further. We calculate the energy consumed by the robot for covering a planar area. The energy-efficiency of a motion plan is defined as the size of covered area per unit energy:

$$\text{energy efficiency} = \frac{\text{size of an area}}{\text{energy to cover the area}} \quad (4)$$

Even though we compare only three strategies, our approach is general and applicable to other motion plan. We calculate the robot's energy by dividing it into three parts: moving at a constant velocity, accelerating and decelerating, and turning.

E. Energy Efficiency of Scan Lines

Suppose the height of the scan lines is h and the width is $2nl$, as shown in Figure 4 (a). This path can be divided into $2n + 1$ line segments: $n + 1$ of length h and n of length $2l$. The robot has to accelerate and decelerate once for each segment so it accelerates $2n + 1$ times. The robot also decelerates $2n+1$ times. The robot turns $2n$ times, $90°$ each time. The scan lines in Figure 4 (a) show the movement of the robot's center. Because the robot covers a distance of l on each side, the covered area is $(2nl + 2l) \times (h + 2l)$.

First, we calculate the energy consumption while the robot moves at a constant velocity along straight lines ($\Omega = 0$). We can find the energy consumed for each line segment. Let $< 0, S, 0 >$ be the velocity when the robot moves upward vertically in Figure 4 (a). The value of S is the peak speed of the robot. The motion for the other directions (downward vertically and horizontally) can be calculated in the same way. Suppose the robot uses a constant acceleration, $< 0, A, 0 >$, to reach the velocity. It takes $\frac{S}{A}$ time to accelerate and the robot moves $\frac{S^2}{2A}$ during acceleration. For simplicity, we assume the deceleration is the opposite of the acceleration, namely $< 0, -A, 0 >$. The robot also moves $\frac{S^2}{2A}$ during deceleration. Consequently, the robot moves at the constant velocity across distance $h - \frac{S^2}{A}$ for $n+1$ vertical segments. For the n horizontal segments, the robot moves across distance $2l - \frac{S^2}{A}$ at a constant velocity, $< -S, 0, 0 >$, if the robot starts from the right corner. The total distance is $(n + 1) \times (h - \frac{S^2}{A}) + n \times (2l - \frac{S^2}{A})$. The time to travel this distance is $\frac{1}{S}[(n+1)(h - \frac{S^2}{A}) + n(2l - \frac{S^2}{A})]$. The power of the motors can be computed by using Formula (3). Let P_S be the power when the robot moves at the constant velocity. Let J_i be $< J_{i,1}, J_{i,2}, J_{i,3} >$ and $\frac{1}{r}J_i < 0, S, 0 >^T$ be the angular velocity of the ith motor. The total energy can be computed by

$$P_S = \sum_{i=1}^{k} P_m(\frac{1}{r}J_i < 0, S, 0 >^T, 0)$$
$$E_1 = P_S \times \frac{1}{S}[(n + 1)(h - \frac{S^2}{A}) + n(2l - \frac{S^2}{A})] \quad (5)$$

If $h < \frac{S^2}{A}$ or $2l < \frac{S^2}{A}$, the robot does not travel at a constant velocity; instead, the robot consumes only acceleration, deceleration, and turning energy. To calculate the energy consumed during acceleration or decelerating, we have to find the instantaneous velocity of the motors. Suppose acceleration starts at time zero, at time t, the robot's velocity is $< 0, At, 0 >$. The ith motor's angular velocity is $\frac{1}{r}J_i < 0, At, 0 >^T$ and the angular acceleration is $\frac{1}{r}J_i < 0, A, 0 >^T$. Its power consumption is $P_m(\frac{1}{r}J_i < 0, At, 0 >^T, \frac{1}{r}J_i < 0, A, 0 >^T)$. Let $P_A(t)$ be the power of all motors at time t, then $P_A(t) = \sum_{i=1}^{k} P_m(\frac{1}{r}J_i < 0, At, 0 >^T, \frac{1}{r}J_i < 0, A, 0 >^T)$. Similarly, we can define the power during deceleration $P_D(t) = \sum_{i=1}^{k} P_m(\frac{1}{r}J_i < 0, S - At, 0 >^T, \frac{1}{r}J_i < 0, -A, 0 >^T)$ The total energy for acceleration and deceleration is

$$E_2 = (2n + 1) \int_0^{\frac{S}{A}} P_A(t)dt$$
$$E_3 = (2n + 1) \int_0^{\frac{S}{A}} P_D(t)dt \quad (6)$$

Last, we compute the energy consumed for turning. We can apply the same technique by dividing it into three parts: turning at a constant velocity, accelerating the angular velocity, and decelerating the angular velocity. Let Ω be the robot's constant angular velocity and Λ be the angular acceleration. The total energy for turning can be calculated using the same approach as shown in Formulas (5) and (6). We need to make four adjustments: (i) replace S by Ω and A by Λ, (ii) change $2n+1$ to $2n$ since there are only $2n$ turns, (iii) change the traveled distance at the constant velocity to the turned angle at the constant angular velocity, and (iv) add them together. Let E_4 be the energy for turning. The energy efficiency is the covered area divided by the total energy:

$$\frac{\text{area}}{\text{energy}} = \frac{(2nl + 2l)(h + 2l)}{E_1 + E_2 + E_3 + E_4} \quad (7)$$

F. Energy Efficiency of Square Spirals

A similar procedure can be used to calculate the energy efficiency of square spirals. In Figure 4 (c), the covered area is $(2nl + 2l)^2$. Notice that the covered areas of square spirals are always square. This is different from scan lines because scan lines cover rectangular areas. There are $2n + 1$ line segments and $2n$ turns. The robot accelerates $2n+1$ times and decelerates $2n+1$ times. The only difference between the scan lines and the square spirals is the length of the line segments: for the square spiral, the lengths gradually increase and are $2l, 2l, 4l, 4l, 6l, 6l, ..., 2nl, 2nl$, and $2nl$. Therefore, E_1 for the square spiral is written as follows:

$$E_1 = \frac{P_S}{S}[(2nl - \frac{S^2}{A}) + 2\sum_{j=1}^{n}(2jl - \frac{S^2}{A})] \quad (8)$$

G. Energy Efficiency of Spirals

A different approach is needed for computing the energy efficiency for spirals. The robot is constantly turning ($\Omega \neq 0$). Let Θ be the angle the robot moves around the center. The length of the path is

$$\int_0^\Theta \rho d\theta = \int_0^\Theta \frac{l}{\pi} \theta d\theta = \frac{l}{2\pi} \Theta^2 \qquad (9)$$

The covered area is

$$2l^2 + \int_{\Theta-2\pi}^\Theta \frac{1}{2}(\rho+l)^2 d\theta = 2l^2 + \int_{\Theta-2\pi}^\Theta \frac{1}{2}(\frac{l}{\pi}\theta+l)^2 d\theta$$
$$= 2l^2 + \frac{\pi l^2}{3} + \frac{l^2\Theta^2}{\pi} \qquad (10)$$

The area $2l^2$ is added for half of the covered tile when the robot stops (the other half tile is included in the integration). The robot moves at velocity $< V_x, V_y, \Omega >$. To make a fair comparison, we assume the robot's linear speed, $\sqrt{V_x^2 + V_y^2}$, is S. When the robot is at location (ρ, θ) using the polar coordinate, the curvature K is $\frac{\pi(\pi^2\rho^2+2l^2)}{(\pi^2\rho^2+l^2)^{\frac{3}{2}}}$ [17]. The robot's angular velocity Ω is KS. The total energy is the integration of all motors' power along the spiral. Due to the limitation of space, we do not derive the formulas in this paper. Interested readers are encouraged to follow the procedure explained earlier to obtain the analytic form of the energy efficiency.

IV. EXPERIMENTS AND SIMULATIONS

We use a commercial mobile robot called Palm Pilot Robot Kit (PPRK) for our experiments; it was originally designed at Carnegie Mellon University [14]. The robot has three polyurethane omnidirectional wheels driven by three MS492MH DC servo motors. Figure 3 shows the top view of the robot. The robot is powered by one 9 V battery for the control circuit and four 1.5 V batteries for the motors. Every motor has three inputs: power, ground, and control. We use a data acquisition (DAQ) card from National Instrument Inc. to measure the current and the voltage of each motor. The DAQ is connected to a laptop computer so that the measurement facility can follow the robot while it is moving. We measure the motor's power at different angular speeds. From our measurement, we construct a sixth-degree polynomial to describe the relationship between a motor's angular velocity and its power consumption. Figure 1 shows that our model closely follows the measured data.

We use simulations to compare the energy efficiency of different scenarios. Our simulator has been validated by comparing the simulated results with data from real measurement with 96% accuracy. For our robot, the distance from each wheel to the robot's center b is

$0.12m$. The radius of each wheel r is $0.02m$. We use the following parameters for our simulations: the covered length l is 1 foot, the height of scan line h is 8 m, the constant speed S is $0.08m/s$, the acceleration A is $0.2m/s^2$, the constant angular velocity Ω is $\frac{2}{3}rad/s$, the angular acceleration Λ is $\frac{5}{3}rad/s^2$. From our simulations, the energy for moving one meter along a straight line is $9.34J$. The energy for turning 90 degree is $2.35J$. These numbers are validated by the real measurement.

Figure 5 shows the energy efficiency of the three routes. When the covered area is very small, scan lines have the best efficiency because the robot moves along one straight line without turning. As the area increases, spirals become better. The reason is that scan lines need to decelerate, turn, and accelerate many times when the covered area is large. For a scan line, the robot has to turn $2n$ times in order to cover area $(2nl + 2l) \times (h + 2l)$. For a large covered area, the efficiency of square spirals is between the efficiency of scan lines and spirals. This is because the robot travels increasingly longer straight lines between turns as the covered area of a square spiral grows. Thus, the overhead of turning decreases. This figure demonstrates the importance of an analytic approach for comparing different paths. Figure 6 shows the efficiency of scan lines for different h when the covered area is $100m^2$. When the area is fixed, increasing h reduces the number of decelerations, turns, and accelerations. As the figure indicates, the efficiency can improves 50% from $0.042m^2/J$ to $0.063m^2/J$.
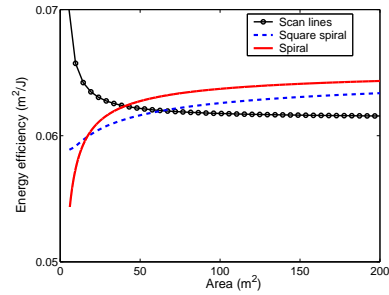

Fig. 5. Energy efficiencies of three paths with different covering area

The energy efficiency is also affected by velocities. Figure 7 shows the energy efficiency at different velocities S for an area of $100m^2$. When S is small, it takes much longer time for the robot to cover this area. Figure 8 shows the time to cover this area. As S increases, the efficiency quickly improves. For spirals, when the velocity S increases from $0.05m/s$ to $0.1m/s$, the energy efficiency increases 51.7% from $0.046m^2/J$ to $0.07m^2/J$. When S is too large, however, the efficiency decreases again. This can be understood from Figure 1.
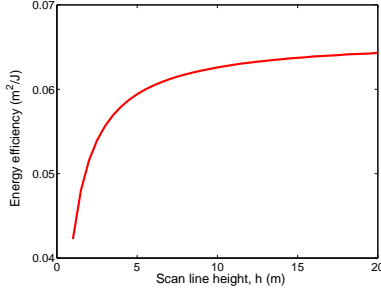
Fig. 6.   Energy efficiencies of the scan lines with different heights

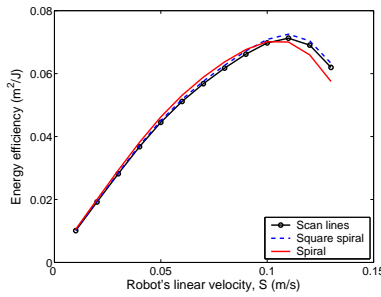The power increases rapidly as the angular velocity of the motor increases above 5 rad/s.

Fig. 7.   Energy efficiencies of three paths with different velocities
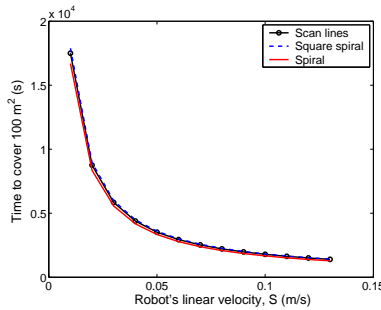

Fig. 8.   Time to cover $100m^2$ with different velocities

While these figures compare the energy efficiency of scenarios with specific parameters, our approach is very general and can be applied to any robot whose motion can be described through a linearly transformation of individual motors.

V. CONCLUSION

This paper presents a general approach finding the energy efficiency of different motion plans. We explain how to use manipulator Jacobian for computing the energy consumption of different plans, including both path plans and velocity schedules. We use simulations to compare the energy efficiency in different scenarios. The energy efficiency depends on the covered areas, the peak speeds, and the paths. For a small area, best energy efficiency is achieved when the robot move along straight lines. When the areas become larger, spirals become the most energy-efficient because the robot can continuously move without stopping and turning. This study provides a foundation for future investigation in conserving the energy consumption of mobile robots.

REFERENCES

[1] J. C. Andreas. *Energy-Efficient Electric Motors*. Marcel Dekker, 2 edition, 1992.
[2] D. J. Balkcom and M. T. Mason.   Extremal Trajectories for Bounded Velocity Differential Drive Robots.   In *ICRA*, pages 2479–2484, 2000.
[3] A. Barili, M. Ceresa, and C. Parisi.   Energy-Saving Motion Control for An Autonomous Mobile Robot.   In *International Symposium on Industrial Electronics*, pages 674–676, 1995.
[4] P. Bertoldi, A. de Almeida, and H. Falkner. *Energy Efficiency Improvements in Electric Motors and Drives*. Springer, 2000.
[5] K.-S. Byun, S.-J. Kim, and J.-B. Song.   Design of A Four-wheeled Omnidirectional Mobile Robot With Variable Wheel Arrangement Mechanism. In *ICRA*, pages 720–725, 2002.
[6] I. Duleba and J. Z. Sasiadek. Nonholonomic Motion Planning Based on Newton Algorithm With Energy Optimization. *IEEE Transactions on Control Systems Technology*, 11(3):355–363, May 2003.
[7] Electro-Craft Corporation.   *DC Motors, Speed Controls, Servo Systems, An Engineering Handbook*. Hopkins, 1973.
[8] K. S. Fu, R. C. Gonzalez, and C. S. G. Lee. *Robotics: Control, Sensing, Vision, and Intelligence*. McGraw-Hill, 1987.
[9] Y. K. Hwang and N. Ahuja. Gross Motion Planning–a Survey. *ACM Computing Surveys*, 24(3):219–291, September 1992.
[10] R. Katoh, O. Ichiyama, T. Yamamoto, and F. Ohkawa. A Real-time Path Planning of Space Manipulator Saving Consumed Energy.   In *International Conference on Industrial Electronics, Control and Instrumentation*, pages 1064–1067, 1994.
[11] B. K. Kim and K. G. Shin.   Suboptimal Control of Industrial Manipulators With A Weighted Minimum Time-Fuel Criterion. *IEEE Transactions on Automatic Control*, 30(1):1–10, January 1985.
[12] Y. Li and G. M. Bone. Are Parallel Manipulators More Energy Efficient. In *International Symposium on Computational Intelligence in Robotics and Automation*, pages 41–46, 2001.
[13] J. Redi and B. Welsh. Energy-Conservation for Tactical Robot Networks. In *IEEE Military Communications Conference Proceedings*, pages 1429–1433, 1999.
[14] G. Reshko, M. T. Mason, and I. R. Nourbakhk. Rapid Prototyping of Small Robots. Technical report, CMU-RI-TR-02-11, Carnegie Mellon University, 2002.
[15] F. M. Silva and J. T. Machado. Energy Analysis During Biped Walking. In *ICRA*, pages 59–64, 1999.
[16] J. Tang, K. Watanabe, and Y. Shiraishi. Design and Traveling Experiment of An Omnidirectional Holonomic Mobile Robot. In *International IROS*, pages 66–73, 1996.
[17] Wolfram. http://mathworld.wolfram.com/curvature.html.
[18] F. Yamasaki, K. Hosoda, and M. Asada. An Energy Consumption Based Control for Humanoid Walking. In *IEEE/RSJ IROS*, pages 2473–2477, 2002.